A bimodal flexible distribution for lifetime data

Ramires, Thiago G.; Ortega, Edwin M. M.; Cordeiro, Gauss M. & HENS, Niel (2016) A bimodal flexible distribution for lifetime data. In: JOURNAL OF STATISTICAL COMPUTATION AND SIMULATION, 86(12), p. 2450-2470.

DOI: 10.1080/00949655.2015.1115047
Handle: http://hdl.handle.net/1942/22560

A bimodal flexible distribution for lifetime data

Thiago G. Ramires
Department of Exact Sciences, University of São Paulo, Brazil

Edwin M.M. Ortega
Department of Exact Sciences, University of São Paulo, Brazil

Gauss M. Cordeiro
Department of Statistics, Federal University of Pernambuco, Brazil

Niel Hens
Interuniversity Institute for Biostatistics and statistical Bioinformatics (I-Biostat), University of Hasselt, Belgium;
Centre for Health Economic Research and Modelling Infectious Diseases, Vaccine and Infectious Disease Institute, University of Antwerp, Belgium

Abstract

A four-parameter extended bimodal lifetime model called the exponentiated log-sinh Cauchy distribution is proposed. It extends the log-sinh Cauchy and folded Cauchy distributions. We derive some of its mathematical properties including explicit expressions for the ordinary moments and generating and quantile functions. The method of maximum likelihood is used to estimate the model parameters. We implement the fit of the model in the GAMLSS package and provide the codes. The flexibility of the model is illustrated by means of three real data sets.
Keywords: Bi-modality; Exponentiated sinh Cauchy distribution; GAMLSS; Lifetime distribution.

1 Introduction

Generalizing lifetime distributions by introducing a few extra shape parameters is an essential method to better explore the skewness and the tails and other properties of the transformed distributions. Following the latest trend, applied statisticians are now able to construct more generalized distributions, which provide better goodness-of-fit measures when fitted to real data rather than by using the classical distributions. The Weibull, log-normal and log-logistic are very popular distributions for modeling lifetime data and phenomenon with unimodal and monotone failure rates. In these cases, they may be chosen because of their negatively and positively skewed density shapes. However, these models do not provide reasonable parametric fits for modeling phenomenon with non-monotone failure rates such as the bathtub shaped and bimodal failure rates, which are common in reliability and biological studies. In this paper, we study a four-parameter generalization of the exponentiated sinh

Cauchy (ESC) distribution on the basis of the sinh Cauchy (SC) model, both proposed by Cooray (2013), for modeling bimodal and unimodal data. The advantage of this approach for constructing a parametric family of distributions lies in its flexibility to model both bathtub and bimodal failure rates even though the baseline failure rate may be monotonic. The generated model is called the *exponentiated log-sinh Cauchy* (ELSC) distribution. As we will see later, its hazard rate function (hrf) can be constant, decreasing, increasing, upside-down bathtub (unimodal), bathtub and bimodal shaped. Due to the great flexibility of the ELSC hrf, it thus provides a good alternative to many existing life distributions in modeling positive real data sets.

Cooray (2013) applied the hyperbolic sine transformation to the standard Cauchy distribution by defining the SC model, whose cumulative density function (cdf) is given by

$$\Pi(y) = \frac{1}{2} + \frac{1}{\pi} \arctan\left[\nu \sinh\left(\frac{y-\mu}{\sigma}\right)\right], \qquad y \in \mathbb{R}, \tag{1}$$

where $\mu \in \mathbb{R}$ and $\sigma > 0$ are the location and scale parameters, respectively, and $\nu > 0$ is the symmetry parameter, which characterizes the bi-modality of the distribution. The SC distribution produces both bimodal and unimodal densities with a wide range of tail weights. It has a real support and therefore is not appropriate for survival data. As a better alternative, we present the *log-sinh Cauchy* (LSC) model.

Let Y be a random variable having cdf (1). The random variable $X = \mathrm{e}^{\mathrm{Y}}$ defines the LSC distribution, whose cdf is given by

$$G(x) = \frac{1}{2} + \frac{1}{\pi} \arctan\left[\nu \sinh\left(\frac{\log(x)-\mu}{\sigma}\right)\right], \qquad x > 0. \tag{2}$$

The SC and LSC models are not appropriate for modeling real data, even though they have some theoretical advantages due to their symmetric nature. To provide an asymmetry for the SC distribution, Cooray (2013) proposed the ESC distribution using the exponentiated class of distributions (Gupta and Kundu, 2001). The cdf of the exponentiated class is given by

$$F(x) = G(x)^{\tau}, \tag{3}$$

where $G(x)$ is the parent cdf and $\tau > 0$ denotes an extra power shape parameter. By differentiating (3), the probability density function (pdf) of the exponentiated class is given by

$$f(x) = \tau G(x)^{\tau-1}\, g(x), \tag{4}$$

where $g(x)$ is the baseline pdf.

The paper is outlined as follows. In Section 2, we define the ELSC model by applying the exponentiated generator to the LSC distribution. In Section 3, we derive a power series for the quantile function (qf) of this distribution. In Section 4, we obtain explicit expressions for its moments. A range of its mathematical properties is explored in Section 5 including generating function, mean deviations and order statistics. The estimation of the model parameters by maximum likelihood is addressed in Section 6. The performance of the maximum likelihood estimators (MLEs) is investigated through a simulation study in Section 7. Applications to three real data sets are addressed in Section 8 to prove

empirically the flexibility of the model. In Section 9, we provide a brief discussion of the template for the ELSC distribution implemented in the "GAMLSS" R package (Stasinopoulos and Rigby, 2007). We also provide the computational codes used in the applications. Finally, Section 10 ends with some conclusions.

2 The ELSC model

We can add skewness for an extended LSC distribution by adopting the exponentiated class of distributions (Gupta and Kundu, 2001) given by (3). Inserting (2) in equation (3), the ELSC cdf is given by

$$F(x;\mu,\sigma,\nu,\tau) = \left\{\frac{1}{2} + \frac{1}{\pi}\arctan\left[\nu\,\sinh\left(w\right)\right]\right\}^{\tau}, \tag{5}$$

where $w = [\log(x) - \mu]/\sigma$. For $\tau = 1$, the LSC distribution is just a special case of (5). The pdf corresponding to (5) is given by

$$f(x;\mu,\sigma,\nu,\tau) = \frac{\tau\nu}{x\,\sigma\,\pi}\,\frac{\cosh\left(w\right)}{\left[\nu^2\,\sinh^2(w)+1\right]}\left\{\frac{1}{2} + \frac{1}{\pi}\arctan\left[\nu\,\sinh(w)\right]\right\}^{\tau-1}. \tag{6}$$

Henceforth, let $X \sim$ELSC(μ,σ,ν,τ) be a random variable with density function (6). We can omit sometimes the dependence on the parameters and and write simply $f(x) = f(x;\mu,\sigma,\nu,\tau)$.

The survival function and hrf of X are given by $S(x) = 1-F(x)$ and $h(x) = f(x)/S(x)$, respectively. Plots of the ELSC density, survival and hazard functions for selected parameter values are displayed in Figures 1, 2 and 3, respectively.

In Figure 1a-b, we check the effects of the location and scale parameters μ and σ on the function $f(x)$. Figure 1c reveals clearly the bi-modality effect caused by the parameter ν. Further, Figure 1d reveals that the density of X is bimodal and symmetric, bimodal and right-skewed, bimodal and left-skewed depending on the parameter τ. Figures 3a and 3b indicate that the hrf of X has decreasing, unimodal and bimodal forms and double bathtub-shaped and unimodal and bathtub-shaped, respectively.

We provide in Figures 4a-b a numerical investigation to identify how the parameter values change the shapes of the hrf of X for some parameter ranges. Based on these plots, we can obtain bimodal shapes for the hrf of X for small values of the parameters ν and τ. However, large values of these parameters are necessary to obtain this characteristic when the parameter σ increases.

Because of the current computational facilities, several researchers construct new lifetime models to facilitate their use in lifetime data analysis. It is a common practical technique to fit new models to real data and develop scripts in statistical software R Team (2013). de Castro *et al.* (2010) implemented some long-term survival models by taking the Weibull as the parent distribution. Rodrigues *et al.* (2009) implemented the COM−Poisson cure rate model and illustrate its flexibility by means of a real data set. Following these ideas, the ELSC model is implemented in the R software, where a short discussion is given in Section 9.

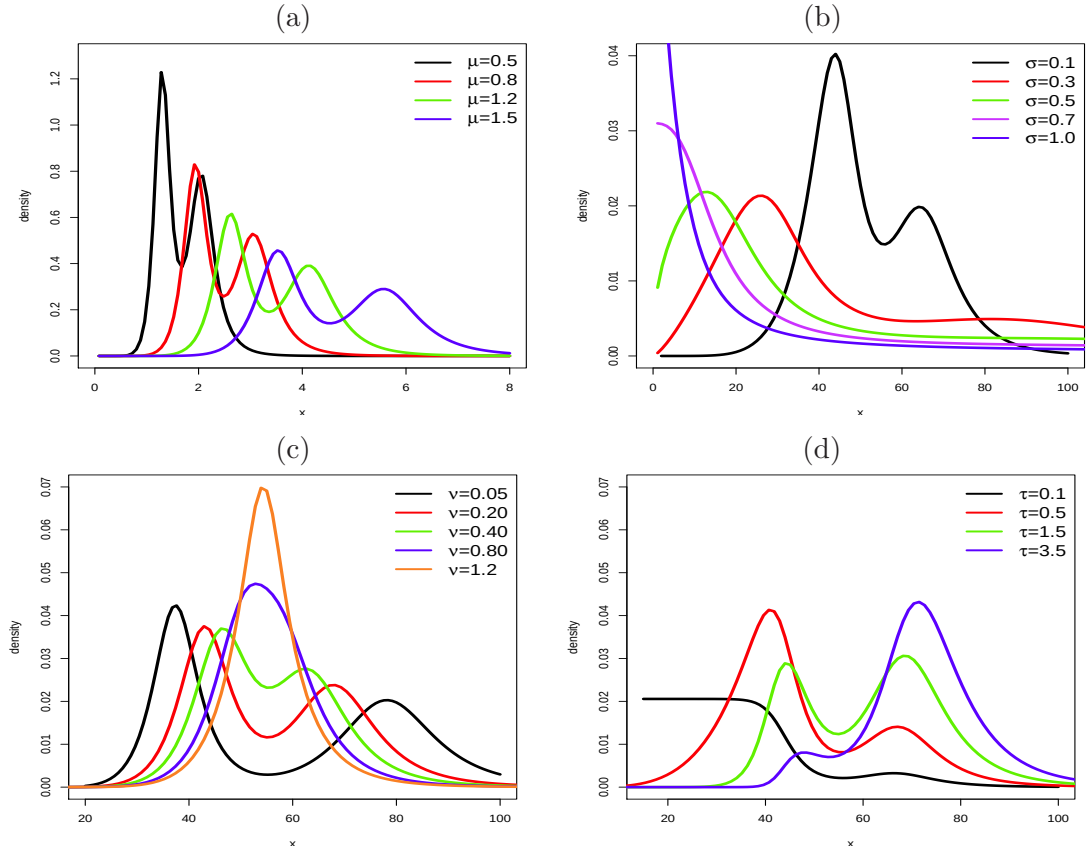

Figure 1: Plots of the ELSC density for fixed values of: (a) $\sigma = 0.1$, $\nu = 0.2$ and $\tau = 1$; (b) $\mu = 4$, $\nu = 0.3$ and $\tau = 0.7$; (c) $\mu = 4$, $\sigma = 0.1$ and $\tau = 1$; (d) $\mu = 4$, $\sigma = 0.1$ and $\nu = 0.2$.

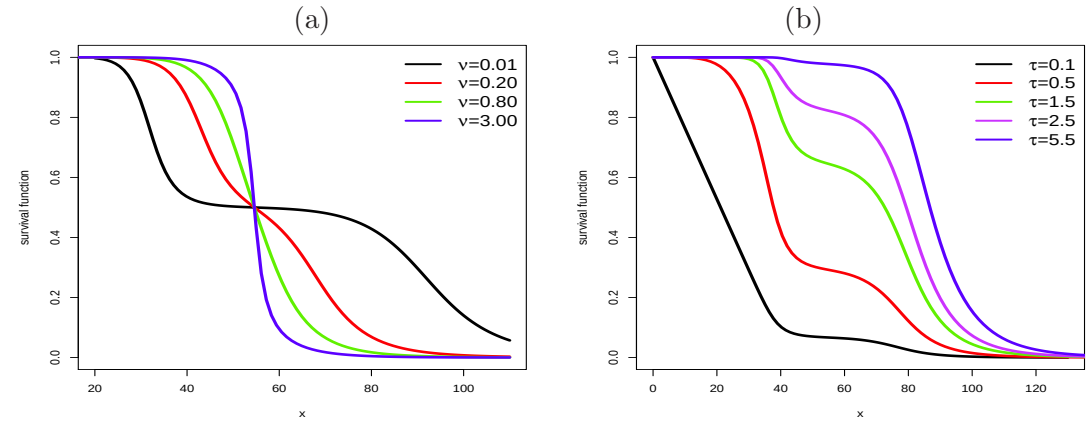

Figure 2: The ELSC survival function when $\mu = 4$, $\sigma = 0.1$ and: (a) For $\tau = 1$ and different values of ν; (b) For $\nu = 0.05$ and different values of τ.

3 Expansion of the quantile function

Inverting $F(x) = u$ (for $0 < u < 1$), we obtain the qf of X

$$x = Q(u) = \exp\left(\mu + \sigma \operatorname{arcsinh}\left\{\frac{1}{\nu}\tan\left[\pi\left(u^{1/\tau} - 0.5\right)\right]\right\}\right). \tag{7}$$

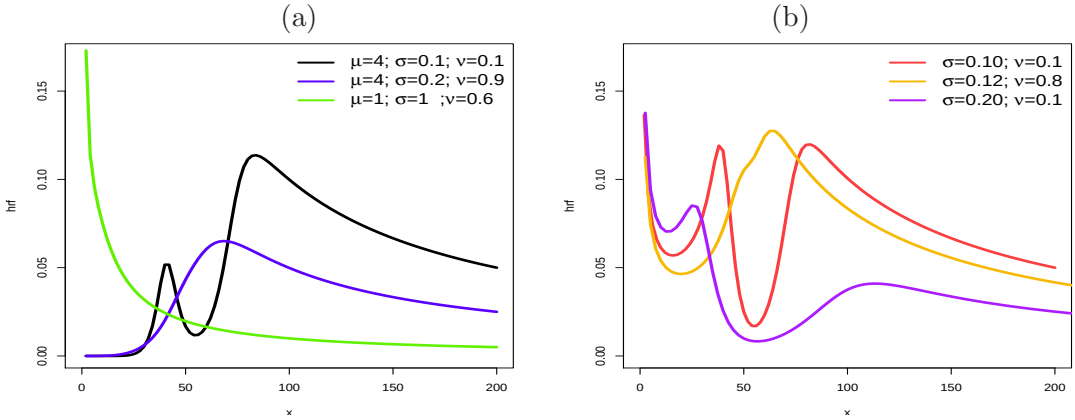

Figure 3: The ELSC hrf: (a) For $\tau = 1$ and different values of μ, σ and ν; (b) For $\mu = 4$ and $\tau = 0.01$ and different values of σ and ν.

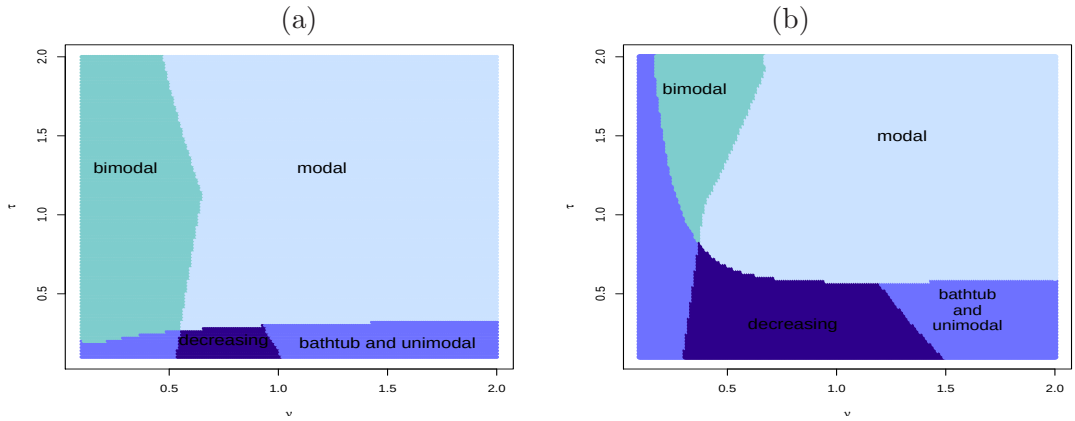

Figure 4: The ELSC hrf shapes as functions of ν and τ for $\mu = 1$ and: (a) $\sigma = 0.4$; (b) $\sigma = 0.7$.

Quantiles of interest can be obtained from (7) by substituting appropriate values for u. In particular, the median of X is obtained when $u = 1/2$. We can also use (7) for simulating ELSC random variables by setting u as a uniform random variable in the unit interval $(0, 1)$. The qf of the LSC distribution can be obtained by taking $\tau = 1$ in equation (7).

Next, we derive an expansion for the qf of X to obtain some ELSC properties in the following sections. Expanding (7) in power series using Mathematica, we obtain

$$Q(u) = \mathrm{e}^{\mu} \exp\left(\sum_{\mathrm{k}=0}^{\infty} \mathrm{c_k}\, \mathrm{z}^{2\mathrm{k}+1}\right),$$

where $z = u^{1/\tau} - 0.5$, $c_k = \frac{\sigma\, b_k}{(2k+1)!}\left(\frac{\pi}{\nu}\right)^{2k+1}$ and $b_0 = 1$, $b_1 = (2\nu^2 - 1)$, $b_2 = (16\nu^4 - 20\nu^2 + 9)$, $b_3 = (272\nu^6 - 616\nu^4 + 630\nu^2 - 225)$, $b_4 = (7936\nu^8 - 28160\nu^6 + 48384\nu^4 - 37800\nu^2 + 11025), \ldots$

By simple transformation of quantities, we can write

$$Q(u) = \mathrm{e}^{\mu} \exp\left(\sum_{\mathrm{k}=1}^{\infty} \frac{\mathrm{d_k}}{\mathrm{k!}}\, \mathrm{z}^{\mathrm{k}}\right), \tag{8}$$

where

$$d_{2j} = 0 \quad \text{for} \quad j = 1, 2, \ldots \qquad \text{and} \qquad d_{2j+1} = (2j+1)!\, c_j \quad \text{for} \quad j = 0, 1, 2, \ldots . \tag{9}$$

We can use the Bell polynomials[1] to rewrite equation (8). The exponential partial Bell polynomials in formal double series expansion are defined by Comtet (1974, p.133) as

$$\exp\left(u \sum_{m \geq 1} x_m \frac{t^m}{m!} \right) = \sum_{n,k \geq 0} \frac{B_{n,k}}{n!}\, t^n\, u^k, \tag{10}$$

where

$$B_{n,k} = B_{n,k}(x_1, x_2, \ldots, x_{n-k+1}) = \sum \frac{n!}{c_1!\, c_2! \ldots (1!)^{c_1} (2!)^{c_2} \ldots}\, x_1^{c_1}\, x_2^{c_2}, \ldots,$$

and the summation is over all integers $c_1, c_2, c_3, \ldots \geq 0$ such that $c_1 + 2c_2 + 3c_3 + \cdots = n$ and $c_1 + c_2 + c_3 + \cdots = k$. These exponential partial Bell polynomials can be evaluated in Mathematica and Maple using **BellY[n,k,{$x_1, \ldots, x_{n-k+1}$}]** and **IncompleteBellB(n, k, x[1], z[2],. . . , x[n-k+1])**.

Using the definition of the complete Bell polynomials and (10), equation (8) can be expressed as

$$Q(u) = \mathrm{e}^{\mu} \sum_{\mathrm{k}=0}^{\infty} \frac{\mathrm{B_k(d_1, \ldots, d_k)}}{\mathrm{k!}}\, \mathrm{z^k},$$

where $B_k = B_k(d_1, \ldots, d_k) = \sum_{r=1}^{k} B_{k,r}(d_1, \ldots, d_{k-r+1})$ (for $k \geq 0$) is the complete Bell polynomial of order k.

The coefficients B_k can be easily obtained using Mathematica, Maple and Sage softwares. Replacing z in the last equation, the qf of X can be rewritten as

$$Q(u) = \mathrm{e}^{\mu} \sum_{\mathrm{k}=0}^{\infty} \frac{\mathrm{B_k(d_1, \ldots, d_k)}}{\mathrm{k!}}\, (\mathrm{u}^{1/\tau} - 0.5)^{\mathrm{k}}. \tag{11}$$

By expanding the binomial term, we have

$$Q(u) = \mathrm{e}^{\mu} \sum_{\mathrm{k}=0}^{\infty} \sum_{\mathrm{j}=0}^{\infty} \frac{(-1)^{\mathrm{k-j}}\, \mathrm{u}^{\mathrm{j}/\tau}}{2^{\mathrm{k-j}}\, \mathrm{k!}} \binom{\mathrm{k}}{\mathrm{j}} \mathrm{B_k(d_1, \ldots, d_k)}.$$

Further, changing $\sum_{k=0}^{\infty} \sum_{j=0}^{\infty}$ by $\sum_{j=0}^{\infty} \sum_{k=j}^{\infty}$, we can write

$$Q(u) = \sum_{j=0}^{\infty} p_j\, u^{j/\tau}, \tag{12}$$

where the coefficients

$$p_j = \mathrm{e}^{\mu} \sum_{\mathrm{k=j}}^{\infty} \frac{(-1)^{\mathrm{k-j}}}{2^{\mathrm{k-j}}\, \mathrm{k!}} \binom{\mathrm{k}}{\mathrm{j}} \mathrm{B_k(d_1, \ldots, d_k)} \tag{13}$$

can be evaluated using the analytical softwares cited before.

[1] `http://en.wikipedia.org/wiki/Bell_polynomials`

Let $W(\cdot)$ be any integrable function in the positive real line. We can write from (6) and (12)

$$\int_0^\infty W(x)\, f(x;\mu,\sigma,\nu,\tau)dx = \int_0^1 W\left(\sum_{j=0}^\infty p_j\, u^{j/\tau}\right) du. \tag{14}$$

Equation (14) is an important result since it allows to obtain various mathematical properties for the ELSC distribution using integrals over $(0,1)$. For the great majority of the applications of (14), we can adopt ten terms in the power series. Equations (12) and (14) are the main results of this section. The formulae derived throughout the paper can be easily handled in most symbolic computation software platforms such as those cited before. They have currently the ability to deal with analytic expressions of formidable size and complexity. Established explicit expressions to evaluate statistical measures can be more efficient than computing them directly by numerical integration.

4 Moments

Some of the most important features and characteristics of a distribution can be studied through moments (e.g., tendency, dispersion, skewness and kurtosis). Using (4), the nth moment of X can be expressed as

$$\mu'_n = E(X^n) = \tau \int_0^\infty x^n\, G(x)^{\tau-1}\, g(x)dx = \tau \int_0^1 Q_{\mathrm{LSC}}(u)^n\, u^{\tau-1}du, \tag{15}$$

where $Q_{\mathrm{LSC}}(u)$ denotes the qf of the LSC distribution.

Here, we give two explicit expressions for μ'_n. For the first one, we use the power series for $Q_{\mathrm{LSC}}(u)^n$, which follows by changing μ by $n\mu$, σ by $n\sigma$ and taking $\tau = 1$ in (11). We have

$$Q_{\mathrm{LSC}}(u)^n = \mathrm{e}^{\mathrm{n}\mu} \sum_{\mathrm{k}=0}^{\infty} \frac{\mathrm{B_k}(\mathrm{d}_1^*,\ldots,\mathrm{d}_\mathrm{k}^*)}{\mathrm{k!}}\, (\mathrm{u}-0.5)^{\mathrm{k}}, \tag{16}$$

where

$$d^*_{2j} = 0 \quad \text{for} \quad j = 1,2,\ldots, \qquad d^*_{2j+1} = (2j+1)!\, c^*_j \quad \text{for} \quad j = 0,1,2,\ldots \tag{17}$$

and $c^*_k = k\,\sigma\, b_k\, \pi^{2k+1}/(2k+1)!$.

Replacing (16) in equation (15), we have

$$\mu'_n = \tau\, \mathrm{e}^{\mathrm{n}\mu} \sum_{\mathrm{k}=0}^{\infty} \frac{\mathrm{B_k}(\mathrm{d}_1^*,\ldots,\mathrm{d}_\mathrm{k}^*)}{\mathrm{k!}} \int_0^1 (\mathrm{u}-0.5)^{\mathrm{k}}\, \mathrm{u}^{\tau-1}\mathrm{du}.$$

Let ${}_2F_1(p,q;r;y) = \sum_{j=0}^\infty (p)_j\,(q)_j\, y^j/[(r)_j\, j!]$ be the hypergeometric function, $(p)_j$ the Pochhammer symbol defined by $(p)_j = p(p+1)\cdots(p+j-1) = \Gamma(p+j)/\Gamma(p) = (-1)^j\Gamma(1-p)/\Gamma(1-p-j)$, and $\Gamma(\cdot)$ the gamma function.

The last equation can be expressed in terms of the hypergeometric function[2] as

$$\mu'_n = \mathrm{e}^{\mathrm{n}\mu} \sum_{\mathrm{k}=0}^{\infty} \frac{(-1)^{\mathrm{k}}}{2^{\mathrm{k}}\,\mathrm{k!}}\; {}_2\mathrm{F}_1(-\mathrm{k},\tau;\tau+1;2)\, \mathrm{B_k}(\mathrm{d}_1^*,\ldots,\mathrm{d}_\mathrm{k}^*). \tag{18}$$

[2]http://mathworld.wolfram.com/HypergeometricFunction.html

The hypergeometric function ${}_2F_1(p,q;r;y)$ can be evaluated from Mathematica and Maple as `HypergeometricPFQ[{p,q},{r},y]` and `Hypergeometric([p,q],[r],y)`, respectively.

The second expression for μ'_n can be determined using (7) and (12) in equation (15) and changing μ by $n\mu$, σ by $n\sigma$ and setting $\tau = 1$. We obtain

$$\mu'_n = \tau \sum_{j=0}^{\infty} \frac{p_j^*}{j+\tau}, \tag{19}$$

where $p_j^* = \mathrm{e}^{\mathrm{n}\mu} \sum_{\mathrm{k=j}}^{\infty} \frac{(-1)^{\mathrm{k-j}}}{2^{\mathrm{k-j}}\,\mathrm{k!}} \binom{\mathrm{k}}{\mathrm{j}} \mathrm{B_k}(\mathrm{d}_1^*, \ldots, \mathrm{d}_\mathrm{k}^*)$ and d_k^* is defined by (17).

Equations (18) and (19) are the main results of this section. The central moments (μ_s) and cumulants (κ_s) of X are determined as $\mu_s = \sum_{k=0}^{p}(-1)^k \binom{s}{k} \mu_1'^s \mu'_{s-k}$ and $\kappa_s = \mu'_s - \sum_{k=1}^{s-1} \binom{s-1}{k-1} \kappa_k \mu'_{s-k}$, respectively, where $\kappa_1 = \mu'_1$. The skewness $\gamma_1 = \kappa_3/\kappa_2^{3/2}$ and kurtosis $\gamma_2 = \kappa_4/\kappa_2^2$ follow from the third and fourth standardized cumulants, respectively.

When these moments do not exist, for example, for the Cauchy, Lévy and Pareto distributions, alternative measures for the skewness and kurtosis, based on qfs, are sometimes more appropriate for these distributions. The measures of skewness $\mathcal{B}$ (Galton, 1883) and kurtosis $\mathcal{M}$ (Moors, 1988) are given by

$$\mathcal{B} = \frac{Q(6/8) + Q(2/8) - 2Q(4/8)}{Q(6/8) - Q(2/8)} \quad \text{and} \quad \mathcal{M} = \frac{Q(7/8) - Q(5/8) + Q(3/8) - Q(1/8)}{Q(6/8) - Q(2/8)},$$

respectively.

For the ELSC and LSC distributions, Galton's skewness and Moors' kurtosis can be computed using the qf (7). Figure 5 displays some plots of the measures $\mathcal{B}$ and $\mathcal{M}$ as functions of the shape and bi-modality parameters. The additional shape parameter τ has substantial effect on the skewness and kurtosis of X.

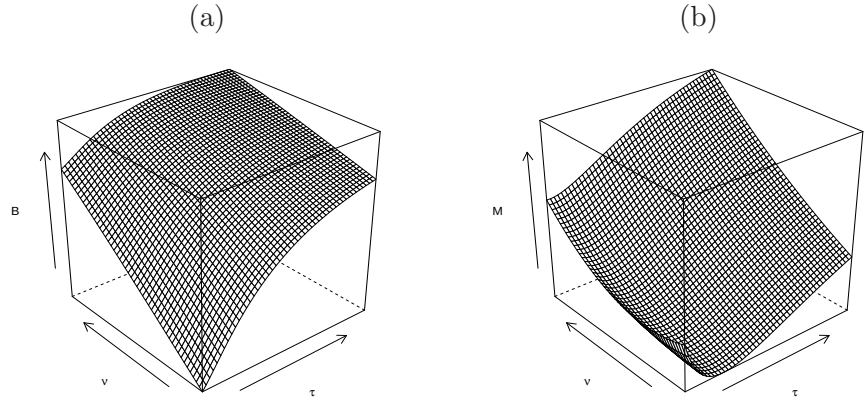

Figure 5: Plots of the measures (a) $\mathcal{B}$ and (b) $\mathcal{M}$ as functions of τ and ν for $\mu = 3$ and $\sigma = 0.2$.

5 Other measures

In this section, we derive the generating function, mean deviations and order statistics of X.

5.1 Generating function

The moment generating function (mgf) $M(t) = \mathrm{E}(\mathrm{e}^{\mathrm{tX}})$ of X can be determined from equation (4) in terms of its qf. We have

$$M(t) = \tau \int_0^\infty \mathrm{e}^{tx}\, G(x)^{\tau-1}\, g(x) dx = \tau \int_0^1 u^{\tau-1} \exp\left[t\, Q_{\mathrm{LSC}}(u)\right] du.$$

Combining equations (8) and (12) when $\tau = 1$, the mgf of X can be written as

$$M(t) = \tau\, \mathrm{e}^{t\, p_0} \int_0^1 u^{\tau-1} \exp\left(\sum_{j=1}^\infty \frac{p_j^{**}\, u^j}{j!}\right) du,$$

where $p_j^{**} = t\, p_j\, j!$ and p_j is given by (13). Using again the complete Bell polynomials, we have

$$\exp\left(\sum_{j=1}^\infty \frac{p_j^{**}\, u^j}{j!}\right) = \sum_{j=0}^\infty \frac{B_j(p_1^{**}, \ldots, p_j^{**})}{j!}\, u^j,$$

and then, the mgf of X follows as

$$M(t) = \tau\, \mathrm{e}^{t\, p_0} \sum_{j=0}^\infty \frac{B_j(p_1^{**}, \ldots, p_j^{**})}{(\tau + j)\, j!}.$$

5.2 Mean deviations

For empirical purposes, the first incomplete moment $m_1(s) = \int_{-\infty}^s x\, f(x)\, dx$ plays an important role for measuring inequality, for example, mean deviations and Lorenz and Bonferroni curves. A formula for $m_1(s)$ follows by setting $u = G(x)$ in (4) as

$$m_1(s) = \tau \int_0^s Q_{\mathrm{LSC}}(u)\, u^{\tau-1} du. \tag{20}$$

Here, we provide two alternatives to compute the first incomplete moment of X. First, $m_1(s)$ can be derived from (18) by taking $n = 1$ as

$$m_1(s) = \tau\, \mathrm{e}^{\mu} \sum_{\mathrm{k}=0}^\infty \frac{(1-2\mathrm{s})^{-\mathrm{k}}\, (\mathrm{s}-0.5)^{\mathrm{k}}\, \mathrm{s}^{\tau}}{\tau\, \mathrm{k}!}\; {}_2\mathrm{F}_1(-\mathrm{k}, \tau; \tau+1; 2\mathrm{s})\, \mathrm{B}_{\mathrm{k}}(\mathrm{d}_1, \ldots, \mathrm{d}_{\mathrm{k}}), \tag{21}$$

where d_k is given by (9). A second formula for $m_1(s)$ can be derived by inserting (12) in equation (20) and setting $\tau = 1$ as

$$m_1(s) = \tau \sum_{j=0}^\infty p_j\, \frac{s^{\tau+j}}{\tau + j}. \tag{22}$$

The main applications of equations (21) or (22) are related to the Bonferroni and Lorenz curves defined (for a given probability π) by $B(\pi) = m_1(q)/(\pi\mu_1')$ and $L(\pi) = m_1(q)/\mu_1'$, respectively, where $\mu_1' = E(X)$ and $q = Q(\pi)$ is the qf of X at π obtained from (7).

The mean deviations about the mean ($\delta_1 = E(|X - \mu_1'|)$) and the median ($\delta_2 = E(|X - M|)$) of X are given by

$$\delta_1(X) = 2\mu_1'\, F(\mu_1') - 2m_1(\mu_1') \qquad \text{and} \qquad \delta_2(X) = \mu_1' - 2m_1(M), \tag{23}$$

respectively, where $M = \mathrm{Median}(X) = Q(0.5)$ is the median, $F(\mu_1')$ is easily evaluated from the cdf (5) and $m_1(z)$ is given by (21) or (22).

5.3 Order statistics

Order statistics make their appearance in many areas of statistical theory and practice. Suppose $X_1, \ldots, X_n$ is a random sample from the ELSC distribution. Let $X_{i:n}$ denote the ith order statistic. Using (5) and (6), the pdf of $X_{i:n}$ can be expressed as

$$\begin{aligned} f_{i:n}(x) &= K\, f(x)\, F(x)^{i-1}\, \{1-F(x)\}^{n-i} = K \sum_{j=0}^{n-i} (-1)^j \binom{n-i}{j} f(x)\, F(x)^{j+i-1} \\ &= K \sum_{j=0}^{n-i} (-1)^j \binom{n-i}{j} \frac{\tau\nu}{x\,\sigma\,\pi} \frac{\cosh(w)}{[\nu^2\,\sinh^2(w)+1]} \left\{ \frac{1}{2} + \frac{1}{\pi} \arctan\left[\nu\,\sinh(w)\right] \right\}^{(j+i)\tau-1}, \end{aligned}$$

where $w = [\log(x) - \mu]/\sigma$ and $K = n!/[(i-1)!(n-i)!]$.

6 Inference

We consider the situation when the time-to-event is not completely observed and is subject to right censoring. Let C_i denote the censoring time. We observe $x_i = \min\{X_i, C_i\}$ and $\delta_i = I(X_i \leq C_i)$, where $\delta_i = 1$ if X_i is a time-to-event and $\delta_i = 0$ if it is right censored (for $i = 1, \ldots, n$). Let c denote the parameter vector of the distribution of the time-to-event. Let X_i be a random variable following (6) with the vector of parameters $\boldsymbol{\gamma} = (\mu, \sigma, \nu, \tau)^T$. From n pairs of times and censoring indicators $(x_1, \delta_1), \ldots, (x_n, \delta_n)$, the log-likelihood function under non-informative censoring is given by

$$\begin{aligned} l(\boldsymbol{\gamma}) &= r[\log(\tau\nu) - \log(\sigma\pi)] - \sum_{i\in F} \log(x_i) + \sum_{i\in F} \log\cosh(w_i) - \sum_{i\in F} \log\left[1 + \nu^2\,\sinh^2(w_i)\right] \\ &+ (\tau-1) \sum_{i\in F} \log\left\{ \frac{1}{2} + \frac{1}{\pi} \arctan[\nu\,\sinh(w_i)] \right\} + \sum_{i\in C} \log\left(1 - \left\{ \frac{1}{2} + \frac{1}{\pi} \arctan\left[\nu\,\sinh\left(w_i\right)\right] \right\}^{\tau} \right), \quad (24) \end{aligned}$$

where r is the number of failures (uncensored observations).

We can obtain the MLE $\widehat{\boldsymbol{\gamma}}$ of $\boldsymbol{\gamma}$ by maximizing the log-likelihood (24) either directly in R using the `optim` function, in SAS using the `NLMixed` procedure and in other statistical software or by solving the nonlinear likelihood equations obtained by differentiating (24). The score functions for the parameters in $\boldsymbol{\gamma}$ are given by

$$U_\mu(\boldsymbol{\gamma}) = -\sum_{i\in F} \frac{\tanh(w_i)}{\sigma} + \sum_{i\in F} \frac{\nu^2\,\sinh(2w_i)}{\sigma\,K_i} + (\tau-1) \sum_{i\in F} \frac{\nu\,\cosh(w_i)}{\pi\sigma\,J_i\,K_i} + \sum_{i\in C} \frac{\tau\nu\,\cosh(w_i)\,J_i^{\tau-1}}{\pi\sigma\,K_i(J_i^\tau - 1)},$$

$$\begin{aligned} U_\sigma(\boldsymbol{\gamma}) &= -\frac{r}{\sigma} - \sum_{i\in F} \frac{w_i}{\sigma} \tanh(w_i) + \sum_{i\in F} \frac{2\nu^2\,w_i}{\sigma\,K_i} \sinh(w_i)\cosh(w_i) + (\tau-1) \sum_{i\in F} \frac{\nu\,w_i}{\pi\,\sigma\,J_i\,K_i} \cosh(w_i) \\ &+ \sum_{i\in C} \frac{\tau\,\nu\,w_i\,J^{\tau-1}}{\pi\,\sigma\,K_i\,(1-J_i^\tau)}\ \cosh(w_i), \end{aligned}$$

$$U_\nu(\boldsymbol{\gamma}) = \frac{r}{\nu} - \sum_{i\in F} \frac{2\nu\,\sinh^2(w_i)}{K_i} + (\tau-1) \sum_{i\in F} \frac{\sinh(w_i)}{\pi\,J_i\,K_i} + \sum_{i\in C} \frac{\tau\,J_i^{\tau-1}\sinh(w_i)}{\pi\,K_i(J_i^\tau - 1)}$$

and

$$U_\tau(\boldsymbol{\gamma}) = \frac{r}{\tau} + \sum_{i \in F} \log(J_i) + \sum_{i \in C} \frac{J_i^\tau}{J_i^\tau - 1} \log(J_i),$$

where $J_i = \frac{1}{2} + \frac{1}{\pi} \arctan[\nu \sinh(w_i)]$ and $K_i = \nu^2 \sinh^2(w_i) + 1$.

The numerical maximization of the log-likelihood function (24) can also be performed in the GAMLSS package in R. The advantage of this package is that we can use many maximization methods, which will depend only on the current fitted model. When there are no explanatory variables or censored observations, we can use the `gamlssML` function for fitting (24) using a non-linear maximization algorithm. When we have censored observations, the additional package `gamlss.cens` is required to determine numerically the observed information of the likelihood function referring to the censored observations. The maximization algorithms adopted in the presence of censored data are the RS and CG procedures. All methods and algorithms are described by Rigby and Stasinopoulos (2005) and Stasinopoulos and Rigby (2007) and they are available in the documentation of the GAMLSS package. The RS algorithm requires the first order derivatives of the logarithm of the density function (6) given in the above equations, and the second order derivatives. The RS method, different from the CG algorithm, does not use the cross derivatives, and thus it is faster for larger data sets. The second order derivatives can be determined numerically in the script discussed in Section 8.

Under standard regularity conditions, the asymptotic distribution of $(\widehat{\boldsymbol{\gamma}} - \boldsymbol{\gamma})$ is $N_4(\mathbf{0}, I(\boldsymbol{\gamma})^{-1})$, where $I(\boldsymbol{\gamma})$ is the expected information matrix. This asymptotic behavior holds if $I(\boldsymbol{\gamma})$ is replaced by $J(\widehat{\boldsymbol{\gamma}})$, i.e., the observed information matrix evaluated at the MLE $\widehat{\boldsymbol{\gamma}}$. Thus, the multivariate normal $N_4(\mathbf{0}, J(\widehat{\boldsymbol{\gamma}})^{-1})$ distribution can be used to construct approximate confidence intervals for the individual parameters.

Further, we can compute the maximum values of the log-likelihoods to obtain the likelihood ratio (LR) statistics for testing some sub-models of the ELSC distribution. For example, the test of $H_0 : \tau = 1$ *versus* $H : \tau \neq 1$ is equivalent to compare the LSC and ELSC distributions. In this case, the LR statistic is given by

$$w = 2\{l(\widehat{\mu}, \widehat{\sigma}, \widehat{\nu}, \widehat{\tau}) - l(\widetilde{\mu}, \widetilde{\sigma}, \widetilde{\nu}, 0)\},$$

where $\widehat{\mu}$, $\widehat{\sigma}$, $\widehat{\nu}$ and $\widehat{\tau}$ are the MLEs under H and $\widetilde{\mu}$, $\widetilde{\sigma}$ and $\widetilde{\nu}$ are the estimates under H_0.

7 Simulation

We simulate the ELSC distribution (for $\mu = 4, \sigma = 0.1, \nu = 0.05, 0.6, 1.2$ and $\tau = 0.5, 1.5, 2$), considering bi-modality and unimodal forms, from equation (7) by using a random variable U having a uniform distribution in $(0, 1)$. We take n=50, 150 and 300 and, for each replication, we calculate the MLEs $\hat{\mu}$, $\hat{\sigma}$, $\hat{\nu}$ and $\hat{\tau}$. We repeat this process $1,000$ times and determine the average estimates (AEs), biases and means squared errors (MSEs). The results of the Monte Carlo study are given in Table 1. They indicate that the MSEs of the MLEs of μ, σ, ν and τ decay toward zero as the sample size increases, as expected under standard asymptotic theory.

We conclude from the figures in Table 1 that the AEs of the parameters tend to be closer to the true parameters when n increases. This fact supports that the asymptotic normal distribution provides an

Table 1: The AEs, biases and MSEs based on 1,000 simulations of the ELSC distribution for μ=4 and σ=0.1, $\nu = 0.05, 0.6, 1.2$ and $\tau = 0.5, 1.5, 2$, and n=50, 150 and 300.

		$\nu = 0.05$ and $\tau = 2$			$\nu = 0.6$ and $\tau = 2$			$\nu = 1.2$ and $\tau = 2$		
n	Parameter	AE	Bias	MSE	AE	Bias	MSE	AE	Bias	MSE
50	μ	4.001	0.001	0.001	2.913	-0.014	0.007	3.987	-0.013	0.003
	σ	0.097	-0.003	0.000	0.095	-0.005	0.001	0.099	-0.001	0.001
	ν	0.048	-0.002	0.001	0.635	0.035	1.371	1.321	0.121	0.433
	τ	2.050	0.050	0.143	2.913	0.913	42.345	2.884	0.884	7.379
150	μ	4.000	0.000	0.000	3.996	-0.004	0.003	3.989	-0.011	0.001
	σ	0.099	-0.001	0.000	0.098	-0.022	0.000	0.100	0.001	0.001
	ν	0.050	0.000	0.000	0.578	-0.022	0.026	1.209	0.009	0.093
	τ	2.014	0.014	0.045	2.181	0.181	1.051	2.368	0.368	1.044
300	μ	4.000	0.000	0.000	3.999	-0.001	0.002	3.996	-0.004	0.001
	σ	0.100	0.000	0.000	0.098	-0.002	0.000	0.100	0.001	0.001
	ν	0.050	0.000	0.000	0.580	-0.020	0.011	1.203	0.003	0.040
	τ	2.008	0.008	0.023	2.062	0.062	0.293	2.145	0.145	0.321
		$\nu = 0.05$ and $\tau = 1.5$			$\nu = 0.6$ and $\tau = 1.5$			$\nu = 1.2$ and $\tau = 1.5$		
n	Parameter	AE	Bias	MSE	AE	Bias	MSE	AE	Bias	MSE
50	μ	4.001	0.001	0.001	3.989	-0.011	0.006	3.990	-0.010	0.003
	σ	0.098	-0.002	0.001	0.097	-0.003	0.001	0.097	-0.003	0.001
	ν	0.050	0.001	0.001	0.581	-0.019	0.089	1.224	0.024	0.351
	τ	1.537	0.037	0.083	1.769	0.269	1.004	1.921	0.421	2.007
150	μ	4.001	0.001	0.001	3.995	-0.005	0.003	3.996	-0.004	0.001
	σ	0.099	-0.001	0.001	0.097	-0.003	0.001	0.101	0.001	0.001
	ν	0.050	0.001	0.001	0.578	-0.022	0.024	1.228	0.028	0.094
	τ	1.508	0.008	0.026	1.610	0.110	0.297	1.631	0.131	0.319
300	μ	4.000	0.001	0.001	3.998	-0.002	0.001	3.998	-0.002	0.001
	σ	0.100	0.001	0.001	0.099	-0.001	0.001	0.099	-0.001	0.001
	ν	0.050	0.001	0.001	0.583	-0.017	0.011	1.197	-0.003	0.040
	τ	1.508	0.008	0.013	1.550	0.050	0.129	1.562	0.062	0.107
		$\nu = 0.05$ and $\tau = 0.5$			$\nu = 0.6$ and $\tau = 0.5$			$\nu = 1.2$ and $\tau = 0.5$		
n	Parameter	AE	Bias	MSE	AE	Bias	MSE	AE	Bias	MSE
50	μ	3.998	-0.002	0.001	3.982	-0.018	0.008	4.003	0.003	0.003
	σ	0.097	-0.003	0.001	0.100	0.000	0.002	0.094	-0.006	0.002
	ν	0.049	-0.001	0.001	0.611	0.011	0.143	1.226	0.026	0.419
	τ	0.503	0.003	0.012	0.578	0.078	0.127	0.498	-0.002	0.075
150	μ	4.000	0.001	0.001	3.990	-0.010	0.003	4.006	0.006	0.001
	σ	0.099	-0.001	0.001	0.101	0.001	0.001	0.097	-0.003	0.001
	ν	0.049	-0.001	0.001	0.600	0.000	0.038	1.200	0.000	0.122
	τ	0.498	-0.002	0.004	0.538	0.038	0.040	0.485	-0.015	0.015
300	μ	4.000	0.001	0.001	3.996	-0.004	0.001	4.002	0.002	0.001
	σ	0.100	0.001	0.001	0.101	0.001	0.001	0.099	-0.001	0.001
	ν	0.050	0.001	0.001	0.602	0.002	0.018	1.205	0.005	0.054
	τ	0.500	0.001	0.002	0.516	0.016	0.015	0.493	-0.007	0.007

adequate approximation to the finite sample distribution of the MLEs. The normal approximation can be oftentimes improved by using bias adjustments to these estimators. Approximations to the their biases in simple models may be determined analytically. Bias correction typically does a very good job for correcting the MLEs. However, it may also increase the MSEs. Whether bias correction is useful in practice depends basically on the shape of the bias function and on the variance of the MLE. In order to improve the accuracy of these estimators using analytical bias reduction one needs to obtain several cumulants of log-likelihood derivatives, which are notoriously cumbersome for the proposed

model. We illustrate the convergence in Figures 6 and 7, where the true densities are given at selected parameter values and the density functions are computed at the AEs given in Table 1 for some sample sizes and $\nu = 0.05$ and $\nu = 0.6$, respectively. In Figures 8 and 9, we present the estimated densities based on $1,000$ samples of the AEs of the parameters μ, σ, τ for $\nu = 0.05$ and $\nu = 0.6$, respectively, and $n = 50, 150$ and 300. These plots are in agreement with the standard asymptotic theory for the MLEs.

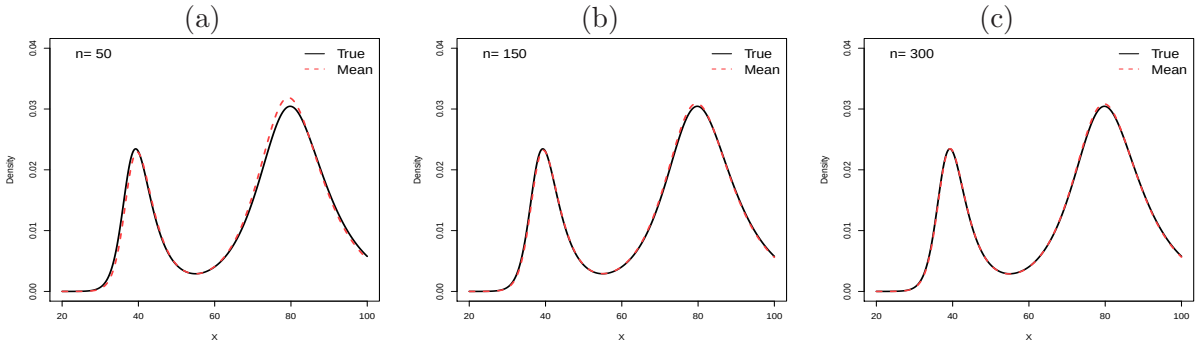

Figure 6: Some ELSC density functions at the true parameter values and at the AEs for μ=4, σ=0.1, ν=0.05 and τ=2 when: (a) n=50; (b) n=150; (c) n=300.

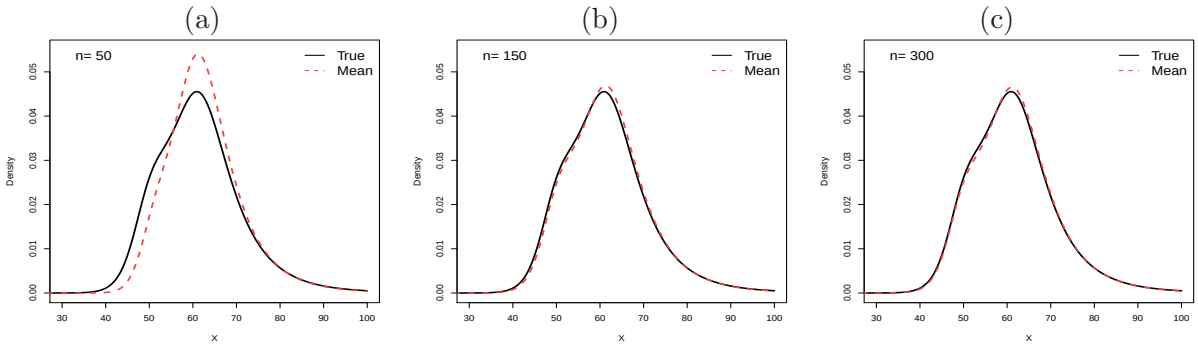

Figure 7: Some ELSC density functions at the true parameter values and at the AEs for μ=4, σ=0.1, ν=0.6 and τ=2 when: (a) n=50; (b) n=150; (c) n=300.

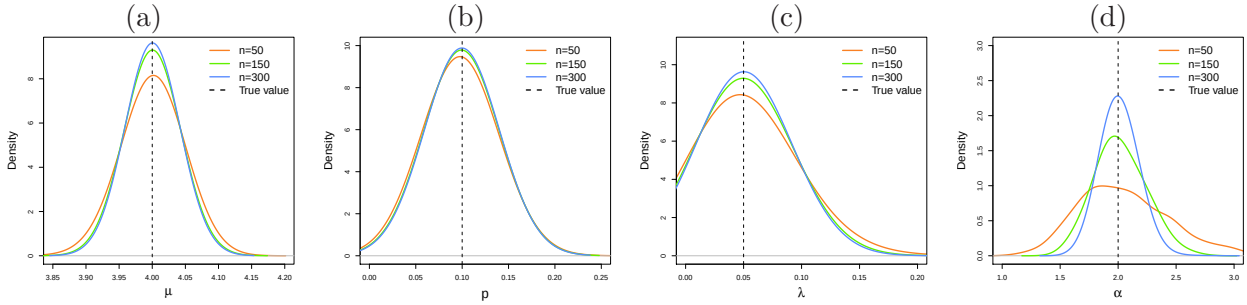

Figure 8: Estimated densities from 1,000 samples for $n = 50, 150, 300$ of the parameters: (a) $\mu = 4$; (b) $\sigma = 0.1$; (c) $\nu = 0.05$; (d) $\tau = 2$ (based on selected parameter values in Table 1 for $\nu = 0.05$)

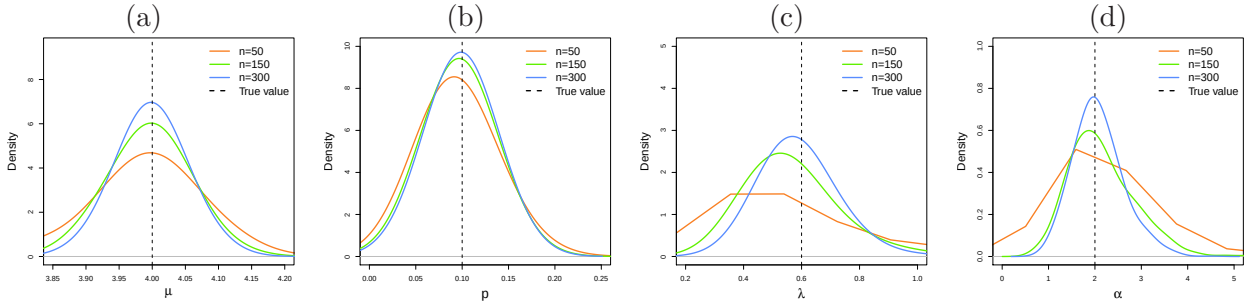

Figure 9: Estimated densities from 1,000 samples for $n = 50, 150, 300$ of the parameters: (a) $\mu = 4$; (b) $\sigma = 0.1$; (c) $\nu = 0.6$; (d) $\tau = 2$ (based on selected parameter values in Table 1 for $\nu = 0.6$)

8 Applications

In this section, we provide three applications to real data to prove empirically the flexibility of the ELSC and LSC models. The computations are performed using the gamlss subroutine in the R software. In the first application, we give an application for bimodal data comparing the ELSC and LSC models with other models implemented in gamlss. In the second application, we show the flexibility of the distribution for censored data and, in the third application, we study the adequacy of the LSC model.

Recently, Cordeiro *et al.* (2014) proposed the McDonald-Weibull (McW) model with scale parameter $\lambda > 0$, shape parameter $\gamma > 0$ and three extra shape parameters $a > 0$, $b > 0$ and $c > 0$. We focus on this model since it extends various distributions previously discussed in the lifetime literature, such as the beta Weibull (BW) (Lee *et al.*, 2007) (for $c = 1$), Kumaraswamy Weibull (KwW) (Cordeiro *et al.*, 2010) (for $a = c$), exponentiated Weibull (EW) (Mudholkar *et al.*, 1995) (for $b = c = 1$), Weibull (for $a = b = c = 1$) and other distributions. Besides of its flexibility, the McW model can take bimodal forms and thus is a competitive model for the ELSC distribution.

All computations in this section are performed using the gamlss subroutine in R and the scripts are described in Section 9.

8.1 Eruption data

First, we provide an analysis of some data on the Old Faithful Geyser in Yellowstone National Park, Wyoming, USA. The data consist of $n = 299$ pairs of measurements referring to the times between the starts of successive eruptions. These data were collected continuously from August 1st until August 15th, 1985; see Azzalini and Bowman (1990) for more details.

We compute the Hartigans' Dip statistic D and its p-value for the test for unimodality. For i.i.d. random variables, the null hypothesis is that X_i has a unimodal distribution. Consequently, the alternative hypothesis is non-unimodal, i.e., at least bimodal. The Dip test can be obtained using a function `dip.test` available in "diptest" R package. More details about the dip test can be obtained in Hartigan and Hartigan (1985). Applying the Dip test to verify that a unimodal distribution would be appropriate to fit the eruption data gives $D = 0.039$ with the p-value 0.002. So, we reject the null hypothesis in favor of a bimodal distribution.

Further, we compare the fits of the ELSC and LSC models with the models available in the gamlss.family package. The `fitDist(..., type=c(''realplus''))` function is used to fit all relevant parametric distributions. The Box-Cox power exponential (BCPEo) distribution is selected as the best model. For details on the distributions available in the package, see Stasinopoulos *et al.* (2014). Table 2 lists the MLEs (and the corresponding standard errors in parentheses) of the model parameters and the values of the Akaike Information Criterion (AIC) and Bayesian Information Criterion (BIC) statistics for the fitted models.

We also evaluate the Cramér-von Mises (W^*) and Anderson-Darling (A^*) statistics described by Chen and Balakrishnan (1995). From a random sample $x_1, \ldots, x_n$ with empirical distribution function $F_n(x)$, the main objective is to test if the sample comes from a specific distribution. The W^* and A^* statistics are given by

$$\begin{aligned} W^* &= \left(n \int_{-\infty}^{+\infty} \{F_n(x) - F(x;\widehat{\boldsymbol{\gamma}}_n)\}^2 dF(x;\widehat{\boldsymbol{\gamma}}_n)\right)\left(1+\frac{0.5}{n}\right) = W^2\left(1+\frac{0.5}{n}\right), \\ A^* &= \left(n \int_{-\infty}^{+\infty} \frac{\{F_n(x) - F(x;\widehat{\boldsymbol{\gamma}}_n)\}^2}{\{F(x;\widehat{\boldsymbol{\gamma}})(1-F(x;\widehat{\boldsymbol{\gamma}}_n))\}} dF(x;\widehat{\boldsymbol{\gamma}}_n)\right)\left(1+\frac{0.75}{n}+\frac{2.25}{n^2}\right), \\ &= A^2\left(1+\frac{0.75}{n}+\frac{2.25}{n^2}\right), \end{aligned}$$

respectively, where $F_n(x)$ is the empirical distribution function and $F(x;\hat{\boldsymbol{\gamma}}_n)$ is the postulated distribution function evaluated at the MLE $\hat{\boldsymbol{\gamma}}_n$ of $\boldsymbol{\gamma}$. The W^* and A^* statistics measure the differences of $F_n(x)$ and $F(x;\hat{\boldsymbol{\gamma}}_n)$. Thus, the lower their values, the more evidence that $F(x;\hat{\boldsymbol{\gamma}}_n)$ generates the sample.

The figures in Table 2 indicate that the ELSC model has the lowest AIC and BIC values among those values of the fitted models, and therefore it could be chosen as the best model. Further, the SEs of the estimates for all fitted models are quite small.

Table 2: MLEs of the model parameters for the eruption data, the corresponding SEs and the AIC and BIC statistics.

Model	μ	σ	ν	τ	AIC	BIC	W^*	A^*
ELSC	4.153	0.069	0.089	1.728	2328.23	2343.03	0.08	0.70
	(0.008)	(0.056)	(0.193)	(0.078)				
LSC	4.193	0.065	0.101	-	2368.26	2379.36	0.32	2.18
	(0.007)	(0.057)	(0.201)	-				
BCPEo	70.675	0.191	0.966	4.973	2387.22	2402.02	0.82	4.36
	(0.014)	(0.032)	(0.271)	(0.143)				

Formal tests for the extra skewness parameters in the ELSC model can be based on the LR statistic described in Section 6. Applying the LR statistic to the eruption data, we reject the null hypothesis $H_0 : \tau = 1$ in favor of the ELSC distribution. The value of the LR statistic is $w = 42.032$ with the p-value < 0.001.

More information is provided by a visual comparison of the histogram of the data with the fitted density functions. The plots of the fitted ELSC, LSC and BCPEo densities and their cdfs are displayed

in Figure 10. The plot of the ELSC hazard rate in Figure 11 reveals that this function has a bimodal shape, small at the first mode and large at the second mode.

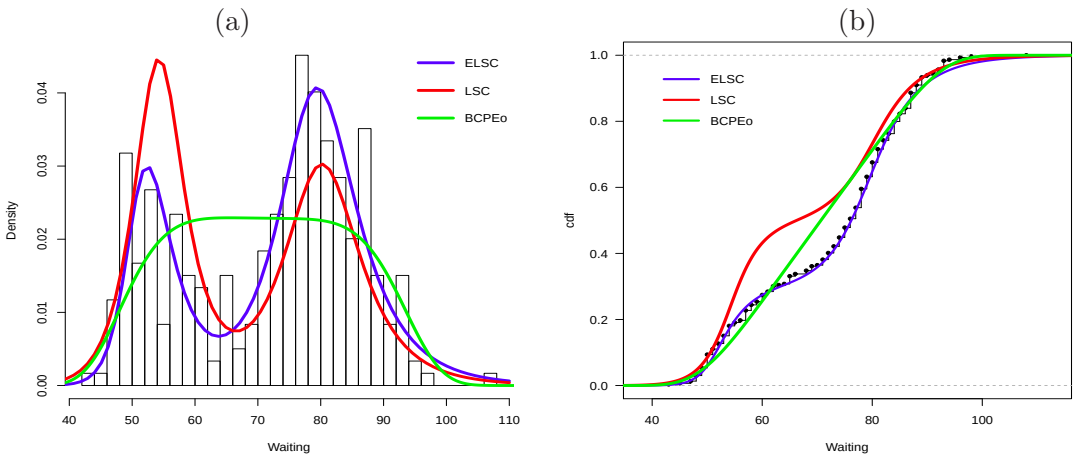

Figure 10: Estimated (a) densities and (b) cdfs for the ELSC, LSC and BCPEo models fitted to the eruption data.

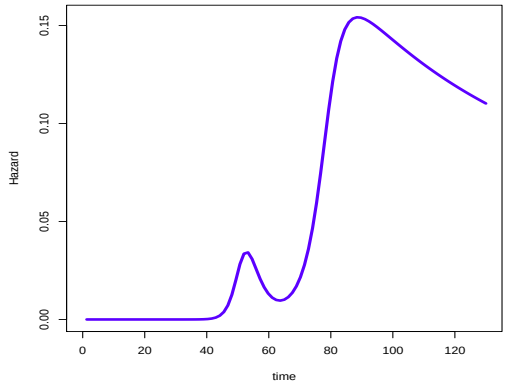

Figure 11: Estimated hrf for the ELSC distribution for eruption data.

8.2 Efron data

Second, we consider the data from a two-arm clinical trial discussed earlier by Efron (1988). Efron noted that the empirical hazard functions for both samples start near zero, suggesting an initial high-risk period at the beginning, a decline for a while, and then stabilization after about one year. He developed and illustrated a methodology for analyzing the data using a combination of techniques of quantal response analysis and the spline regression methods. Specifically, Efron's data from a head and neck cancer clinical trial consist of survival times of 51 patients in arm A who were given radiation therapy and 45 patients in arm B who were given radiation plus chemotherapy. Nine patients in arm A and 14 patients in arm B were lost to follow-up and were regarded as censored.

Cordeiro *et al.* (2014) fitted the McW regression model to these data and noted that it provides a good fit. Here, we consider only the survival times in days x_i and compare the results of the fits of the McW, ELSC and LSC models. Table 3 gives the MLEs (and the corresponding standard errors in parentheses) of the parameters and the values of the AIC and BIC statistics. They indicate that the ELSC model has the lowest values of these statistics among the values of the other fitted models, and therefore it could be chosen as the best model.

Table 3: MLEs of the model parameters for Efron data, the corresponding SEs (given in parentheses) and the AIC and BIC statistics.

Model	μ	σ	ν	τ		AIC	BIC
ELSC	4.788	2.080	2.794	2.308		*1063.9*	*1074.1*
	(0.083)	(0.135)	(0.129)	(0.097)			
LSC	6.141	0.494	0.215	1		1074.4	1082.1
	(0.102)	(0.061)	(0.151)	-			
	λ	γ	a	b	c	AIC	BIC
McW	0.092	0.101	74.352	21.126	0.067	1088.5	1101.3
	(0.028)	(0.008)	(0.655)	(0.192)	(0.001)		
BW	0.281	0.062	167.450	60.159	1	1086.1	1096.3
	(0.106)	(0.005)	(0.406)	(0.177)	-		

By comparing the fits of the ELSC and LSC models using the LR statistic, we reject the null hypothesis $H_0 : \tau = 1$ in favor of the ELSC distribution. The LR statistic is $w = 12.552$ with the p-value < 0.001. Next, we compare the fits of the McW and BW models using the LR statistic. Applying the LR statistic for testing the null hypothesis $H_0 : c = 1$, we obtain $w = 0.00039$ with the p-value almost one. So, we could not reject the BW distribution to fit these data.

The plots of the fitted ELSC, LSC and BW densities and their estimated survival functions are displayed in Figure 12 for the current data ignoring censored observations. Clearly, the ELSC density provides a closer fit to the histogram of the data and the corresponding estimated survival function to the empirical survival function than the other models. The plot of the ELSC hrf in Figure 13 reveals that it has a modal shape.

8.3 Entomology data

Third, we consider the data from a study carried out at the Department of Entomology of the Luiz de Queiroz School of Agriculture, University of São Paulo, which aim to assess the longevity of the mediterranean fruit fly (ceratitis capitata). The need for this fly to seek food just after emerging from the larval stage has permitted the use of toxic baits for its management in Brazilian orchards for at least fifty years. This pest control technique consists of using small portions of food laced with an insecticide, generally an organophosphate, that quickly kills the flies, instead of using an insecticide alone. Recently, there have been reports of the insecticidal effect of extracts of the neem tree leading to proposals to adopt various extracts (aqueous extract of the seeds, methanol extract of the leaves and dichloromethane extract of the branches) to control pests such as the mediterranean fruit fly. For

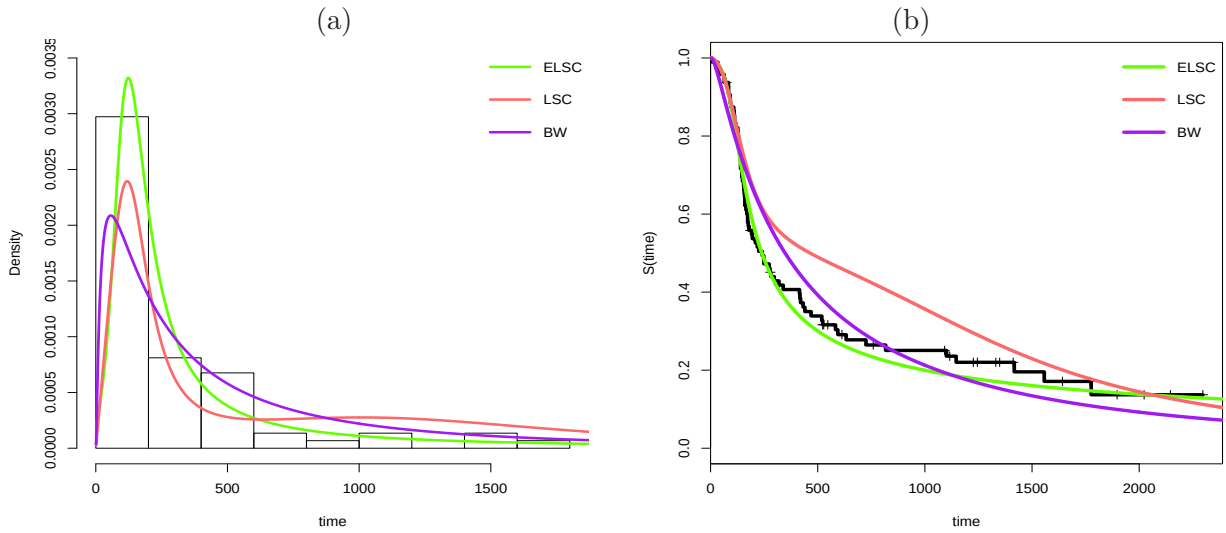

Figure 12: (a) Estimated ELSC, LSC and BW densities for Efron data. (b) Estimated ELSC and LSC survival functions and the empirical survival for Efron data.

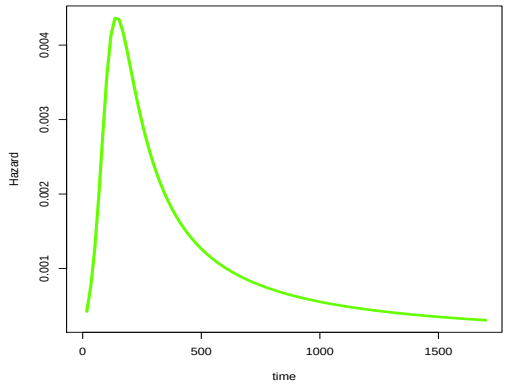

Figure 13: Estimated ELSC hazard function for Efron data.

more details, see Silva *et al.* (2013).

The response variable in the experiment is the lifetime of the adult flies in days after exposure to the treatments. The experimental period was set at 51 days, so that the numbers of larvae that survived beyond this period are considered as censored observations. The total sample size is $n = 72$ because four cases are lost. Therefore, the variables used in this study are: x_i-lifetime of ceratitis capitata adults in days and δ_i-censoring indicator.

Recently, Lanjoni (2013) fitted the Burr XII geometric type II (BXIIGII) distribution to these data and noted that it gives a better fit than the special Burr XII model. Now, we compare the McW and BXIIGII distributions and some of their sub-models with the ELSC and LSC models. For some fitted models, Table 4 provides the MLEs (and the corresponding standard errors in parentheses) of the parameters and the values of the AIC and BIC statistics. The computations are performed using the gamlss subroutine in R. They indicate that the LSC model has the lowest AIC and BIC values

among those values of the fitted models, and therefore it could be chosen as the best model. The LSC model is not able to capture asymmetry but it has the bi-modality characteristic.

Table 4: MLEs of the model parameters for the entomology data, the corresponding SEs (given in parentheses) and the AIC and BIC statistics.

Model	μ	σ	ν	τ		AIC	BIC
ELSC	3.018	0.852	3.367	0.907		1249.0	1261.5
	(0.027)	(0.091)	(0.107)	(0.075)			
LSC	2.998	0.946	3.592	1		*1247.7*	*1257.1*
	(0.029)	(0.101)	(0.106)	-			
	s	c	k	p		AIC	BIC
BXIIGII	14.353	1.164	4.414	0.981		1270.1	1282.7
	(8.175)	(0.389)	(2.532)	(0.0211)			
BXII	34.423	2.214	2.676	1		1282.7	1292.1
	(10.386)	(0.232)	(1.284)	-			
	λ	γ	a	b	c	AIC	BIC
McW	0.079	1.718	0.883	0.329	0.049	1290.0	1305.8
	(0.007)	(0.223)	(0.313)	(0.114)	(0.013)		
BW	0.055	1.608	1.240	0.688	1	1289.7	1302.3
	(0.017)	(0.226)	(0.314)	(0.313)	-		
KwW	0.015	1.133	1	8.787	1.776	1288.9	1301.5
	(0.004)	(0.447)	-	(0.299)	(0.920)	-	
EW	0.044	1.587	1.254	1	1	1287.5	1296.9
	(0.007)	(0.275)	(0.368)	-	-		
Weibull	0.0400	1.797	1	1	1	1286.1	1292.4
	(0.002)	(0.111)	-	-	-		

In order to assess if the model is appropriate, Figure 14a displays the empirical and estimated cumulative distributions for the fitted ELSC and LSC models to the current data. Further, Figure 14b gives the plots of the empirical survival function and the estimated ELSC and LSC survival functions. They indicate the LSC model provides a good fit to these data. Further, using the LR statistic to compare the fits of these models, i.e. for testing the null hypothesis $H_0 : \tau = 1$, we obtain $w = 0.748$ with the p-value= 0.387 and then we could accept the LSC distribution. The plot of its hrf in Figure 15 reveals a modal shape.

9 Program description

The ELSC model is implemented in the gamlss function, which is fully documented in the gamlss package (Stasinopoulos and Rigby, 2007). Here, we will omit several functions for the gamlss package and present only the functions related to the ELSC distribution and its fit to a data set. The computational codes for the ELSC model can be downloaded from `http://goo.gl/yzvoIZ`. The cdf (5) and pdf (6) can be obtained using `dELSC` and `pELSC` functions, respectively. The qf given by (7) can be

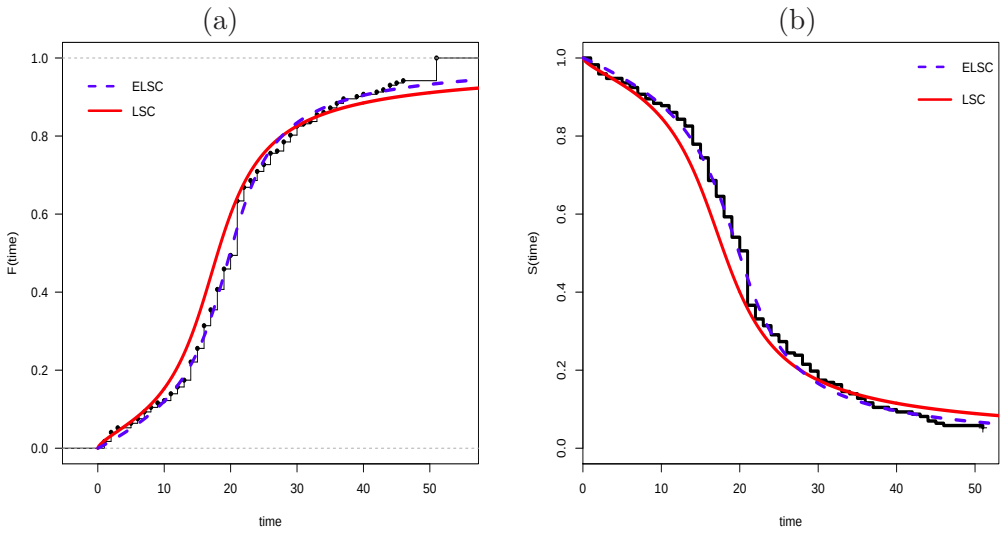

Figure 14: (a) Estimated ELSC and LSC cdfs for entomology data. (b) Estimated ELSC and LSC survival functions and the empirical survival for the entomology data.

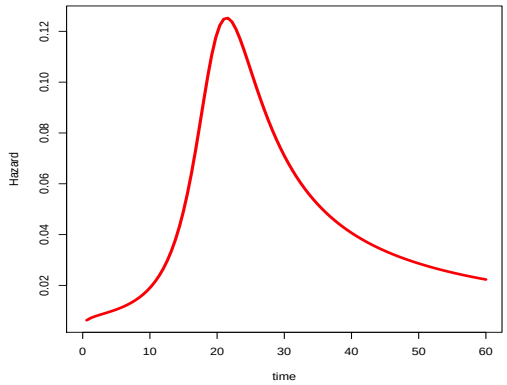

Figure 15: Estimated LSC hazard function for entomology data.

obtained using the `qELSC` function and samples of the ELSC model can be generated using the `rELSC` function. We can use the functions listed above for the LSC sub-model by setting $\tau = 1$ with the `tau.fix=TRUE` function. To optimize the computational time, we can change the initial values of the parameters using the `parameter.fix` function. Otherwise, we can increase the number of interactions using the `n.cyc` function. The fit of the ELSC model to censored data can be performed using the additional package gamlss.cens. The structure of the gamlss function is familiar to users of the R syntax (the glm function, in particular).

10 Conclusions

The paper proposes the exponentiated log-sinh Cauchy (ELSC) distribution that can be used as an alternative to mixture distributions in modeling bimodal data. Various mathematical properties of

the ELSC distribution are investigated. We show that it can accommodate various shapes of the skewness, kurtosis and bi-modality. Its model parameters are estimated by maximum likelihood. Some numerical experiments reveal that the maximum likelihood estimation procedure performs well. Three real data examples prove empirically that the ELSC distribution is very flexible, parsimonious, and a competitive model that deserves to be added to existing distributions in modeling bimodal data. The ELSC model can be fitted using the gamlss package described to facilitate its practical use by researchers from other areas.

References

Azzalini, A. and Bowman, A.W. (1990). A look at some data on the Old Faithful geyser. *Applied Statistics*, 357–365.

Chen, G. and Balakrishnan, N. (1995). A general purpose approximate goodness-of-fit test. *Journal of Quality Technology*, **27**, 154–161.

Comtet, L. (1974). Advanced Combinatorics. D. Reidel Publishing Co., Dordrechet.

Cooray, K. (2013). Exponentiated Sinh Cauchy Distribution with Applications. *Communications in Statistics-Theory and Methods*, **42**, 3838–3852.

Cordeiro, G.M., Ortega, E.M.M. and Nadarajah, S. (2010). The Kumaraswamy Weibull distribution with application to failure data. *Journal of the Franklin Institute*, **347**, 1399–1429.

Cordeiro, G.M., Hashimoto, E.M. and Ortega, E.M. (2014). The McDonald Weibull model. *Statistics*, 48, 256–278.

de Castro, M., Cancho, V.G. and Rodrigues, J. (2010). A hands-on approach for fitting long-term survival models under the GAMLSS framework. *Computer methods and programs in biomedicine*, 97, 168–177.

Efron, B. (1988). Logistic regression, survival analysis, and the Kaplan-Meier curve. *Journal of the American Statistical Association*, 83, 414–425.

Galton, F. (1883). Inquiries Into the Human Faculty & Its Development.

Gupta, R.D. and Kundu, D. (2001). Exponentiated exponential family: an alternative to gamma and Weibull distributions. *Biometrical journal*, **43**, 117–130.

Hartigan, J.A. and Hartigan, P.M. (1985). The dip test of unimodality. *The Annals of Statistics*, 70–84.

Lanjoni, B.R. (2013). O modelo Burr XII geométrico: propriedades e aplicações. Master's Dissertation, Escola Superior de Agricultura Luiz de Queiroz, University of São Paulo, Piracicaba. Retrieved 2015-05-27, from http://www.teses.usp.br/teses/disponiveis/11/11134/tde-17122013-085812/.

Lee, C., Famoye, F. and Olumolade, O. (2007). Beta Weibull distribution: some properties and applications to censored data. *Journal of Modern Applied Statistical Methods*, **6**, 173–186.

Moors, J.J.A. (1988). A quantile alternative for kurtosis. *The statistician*, 25–32.

Mudholkar, G.S., Srivastava, D.K. and Freimer, M. (1995). The exponentiated Weibull family: A reanalysis of the bus-motor-failure data. *Technometrics*, **37**, 436–445.

Rigby, R.A. and Stasinopoulos, D.M. (2005). Generalized additive models for location, scale and shape. *Journal of the Royal Statistical Society: Series C (Applied Statistics)*, **54**, 507–554.

Rodrigues, J., de Castro, M., Cancho, V.G. and Balakrishnan, N. (2009). COM−Poisson cure rate survival models and an application to a cutaneous melanoma data. *Journal of Statistical Planning and Inference*, **139**, 3605–3611.

Silva, M.A., Bezerra-Silva, G.C.D., Vendramim, J.D. and Mastrangelo, T. (2013). Sublethal effect of neem extract on Mediterranean fruit fly adults. *Revista Brasileira de Fruticultura,* **35**, 93-101.

Stasinopoulos, D.M. and Rigby, R.A. (2007). Generalized additive models for location scale and shape (GAMLSS) in R. *Journal of Statistical Software*, **23**, 1–46.

Stasinopoulos, D.M., Rigby, R.A., Akantziliotou, C., Heller, G., Ospina, R., Voudouris, M.D., ... and Stasinopoulos, M.M. (2014). Package "gamlss.dist".

Team, R.C. (2000). R Language Definition.